Journal of Biomaterials Science, Polymer Edition

ISSN: (Print) (Online) Journal homepage: https://www.tandfonline.com/loi/tbsp20

# A study on optical and thermal properties of natural polymer-based hemicellulose compounds

Hina Abid, Shahzad Maqsood Khan & Saeed Iqbal

**To cite this article:** Hina Abid, Shahzad Maqsood Khan & Saeed Iqbal (2021): A study on optical and thermal properties of natural polymer-based hemicellulose compounds, Journal of Biomaterials Science, Polymer Edition, DOI: 10.1080/09205063.2021.1925392

**To link to this article:** https://doi.org/10.1080/09205063.2021.1925392

Published online: 07 Jun 2021.

JOURNAL OF BIOMATERIALS SCIENCE, POLYMER EDITION
https://doi.org/10.1080/09205063.2021.1925392



# A study on optical and thermal properties of natural polymer-based hemicellulose compounds

Hina Abid[a], Shahzad Maqsood Khan[b] and Saeed Iqbal[a]

[a]Department of Chemistry, Forman Christian College, A Chartered University, Lahore, Pakistan;
[b]Institute of Polymer and Textile Engineering, University of the Punjab, Lahore, Pakistan

**ABSTRACT**

Films of husks of *Plantango ovate, Cydonia oblonga, Mimosa pudica, Cochlospermum religiosum* were prepared, delignified without protein and cellulose content, and their optical properties were evaluated. UV-Vis, FTIR TGA analysis revealed that these natural materials have strong potential in fiber optics, contact lenses and human transplantation infrastructure applications, where there is need of efficient transparency, high thermal stability and good conductivity with minimum light absorption. These natural polymeric films possess significant direct and indirect optical band gap values and better optical conductivity than currently in use synthetic polymeric materials. The Refractive index of these films is also found high in the visible region in comparison to pure or composite metal-doped synthetic films. Urbach energy (Eu), Dispersion energy (Ed), Average oscillation wavelength ($\lambda_0$), and oscillation strength($S_0$) of this hemicellulose based natural polymeric films were found to be appropriate for such optical materials which are green, organic, economical and compatible to human systems.

**ARTICLE HISTORY**
Received 3 March 2021
Accepted 29 April 2021

**KEYWORDS**
Hemicellulose; natural polymers; optical study; polymeric films

## Introduction

In 1953 Franz Urbach presented the idea of Urbach's rule to explain the optical properties of metal halides [1]. Similarly, Magnum Opus reported some optical properties of polymers but to date, limited information is reported regarding Urbach's energy of polymers particularly natural polymers. The history of polymers is about 100 years old; the first nitrocellulose-based natural plastic was obtained in 1862 by the Parkes [2]. Polymers are very dynamic and diverse in their properties that's why they show an extensive range of features with little variation in reagents [3–7]. Various natural polymers like collagen [8] alginate [9] Polysaccharides in the form of chitosan [10] cellulose [11] starch [12] and glycosaminoglycans as hyaluronic acid [13] have been used in many applications.

Hydrogels are soft and absorptive polymer networks that can hold a huge quantity of water with the retention of its shape in water used as a disperse medium [14]. One

CONTACT Hina Abid hinaabid@fccollege.edu.pk Department of Chemistry, Forman Christian College, A Chartered University, Lahore 54000, Pakistan.

of the unique features of hydrogels is its similarity with human soft tissue which makes hydrogels as a promising candidate for biomedical use [15–18] such as in gene vectors, [19] tissue engineering, [20,21] biosensors, [22,23] and cosmetic industry [24]. These application demands excellent biocompatibility and controlled biodegradability of hydrogels. As natural polymer hydrogels are more biocompatible, and biodegradable than synthetic polymer-based hydrogels, that is why they have remarkable potential in biomedical fields [25–30]. Several natural polymers are widely available in plants, animals, and organisms having high molecular weight compounds with a linear long-chain produced by repeating units as a basic structure [31–38].

Hemicelluloses are hetero-polysaccharide compounds. Various sugar units with different substituents make hetero-polymeric chains of polysaccharides. Their chain are shorter than the chain length of cellulose [39]. Several agricultural residues contain approximately 20-30% hemicelluloses, it is the second most abundant biopolymer found in nature. Due to nontoxicity, structure versatility, hydrophilicity and great tendency for chemical modification make the hemicellulose as likely material for multiple applications such as in agriculture land for slow release of fertilizers, biomimetic mineralization and as biosensors [40] There are multiple methods to segregate the hemicellulose from rest of biomass material but each method hold certain limitations associated with it such as acid pretreatments (using strong mineral acids can degrade the sugars) liquid hot water extraction (can cleave the functional groups) Ionic liquid method (could give us high purity but required extensive processing) that is why alkaline extraction method is well studied and broadly used method. As for the synthesis of hydrogels and film alkaline extraction is extremely important to extract hemicellulose from rest of biomass [41]

Films obtained from the seeds and husk of *Plantango ovate, Cydonia oblonga, Mimosa pudica,* and *Cochlospermum religiosum* are studied in this article. Diversity in properties of natural polymers is due to variation in adopted mode of purification and because of chemical properties of added reagents. Thermal and optical properties of the addressed polymers are magnificently suitable for optical applications and the scarcity of information on these properties of natural polymeric films is the motivation of this article.

Aim of this research is to extract and synthesize most appropriate, human compatible and economical raw materials to use in the field of fiber optics, ophthalmic lenses and for encapsulation of various drugs for their controlled release.

## Experimental

### Method

The husk of *Plantango ovate, Cydonia oblonga, Mimosa pudica, Cochlospermum religiosum* were purchased from the local market of Lahore, Pakistan. All the samples were taken and soaked overnight into distilled water (approximately 10 g in 1000 mL) in dark to for maximum absorption of water in plants husks and seeds. The volume of the material is enhanced multiple times by addition of water and then turned into mucilaginous mass. After 24 h of soaking, the upper layer of the mucilaginous mass was decanted off into a separate container and blended using Black and Decker

Figure 1. Raw film obtained before delignification.

Model Germany Blender for 5 to 10 min to homogenize the material uniformly. Afterward, blended mucilaginous material was left intact for ten minutes. The mucilaginous mass was filtered using 3 to 4 folds of Muslin Cloth as filter media to remove all fibers and suspended impurities. After filtration the mucilaginous material was spread over the polyethylene sheets in polypropylene trays to turn into the uniform film by drying under persistent cold air. Once films were formed, it was observed that these films still possess certain color substances due to the presence of lignin content in the materials which is present naturally in hemicellulose materials.

The films were then submerged into the solution of 10% solution of sodium sulfite (optimized the concentration according to the nature of films obtained) using alkaline extraction [40] in order to remove cellulose and lignin. The solution was then agitated continuously for 8 to 10 h using magnetic stirrer LabTech Korea. Subsequently, mucilaginous mass was then washed with water and ethanol respectively and spread again on polyethylene sheets in polypropylene trays to get transparent films. This process was repeated for multiple times till transparent pure hemicellulose films were obtained (Figure 1).

## Characterization

### Fourier transform infra-red spectroscopy (FTIR)

The FT-IR spectra were recorded in using Agilent Technologies Cary 630 FTIR in Transmission Mode at the wave number range 4000 to 630 $cm^{-1}$.

### Thermogravimetric analysis (TGA)

The TGA/DSC data was recorded using Thermogravimetric analyzer SDT Q600 TA Instrument USA. from ambient temperature to 800 Degree Celsius by using temperature ramp of 20 °C/min in the presence of 10 mL/minute Nitrogen supply for inert atmosphere for the evaluation of the pyrolysis weight loss.

## Optical studies

Optical studies of the prepared films were performed by using UV spectrophotometer Model Make. The UV-Visible spectra were recorded in Absorption and Transmission

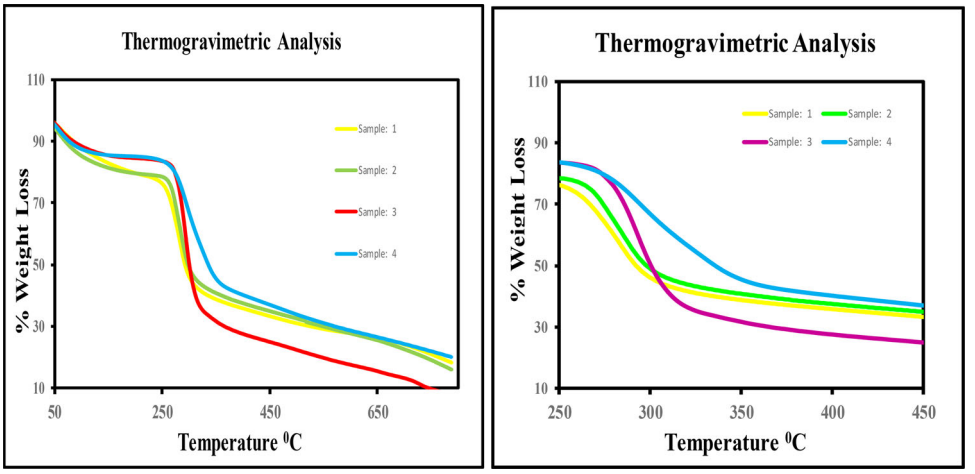


**Figure 2.** FTIR of *Plantango ovate, Cydonia oblonga, Mimosa pudica, and Cochlospermum religiosum*.

mode at the wavelength from 200 nm to 800 nm. Using UV visible absorbance values UV-Visible Absorption and Transmittance Spectra was analyzed, and Optical Energy Band Gap, Refractive Index, Optical Dispersion Parameters, Optical Conductivity and Urbach Energy were calculated.

## Results and discussion

### *FTIR studies*

The FTIR spectra of films prepared after extraction of materials from husks of *Plantango ovate, Plantango ovate, Cydonia oblonga, Mimosa pudica, Cochlospermum religiosu plants* are shown in the Figure 2. The characteristic wavelength around 1246 nm is because of hemicellulose structure correspond to C–H stretching and deformation of $-CH_3$. Absorptions in the region of 1400–1660 nm are associated with O–H stretching. As for lignin, the characteristic wavelength of 1404 nm is disappeared due to the delignification of the all four samples. The wavelengths of 1600 nm and 1725 nm relate to C–H vibration. A distinct peak at 1148 nm is due to glycosidic linkage in polysaccharides. The signal approximately 1725 nm, which appears is for hemicellulose may relate to the C–H stretching of $-CH_2$. The common characteristic wavelengths of near 1800 approximately 1725 nm are recognized to CO stretching of $-CO_2H$ and the combination of O–H stretching and deformation vibrations. The signal around 2100 nm is connected with the combination of O–H and C–H stretching vibrations for hemicellulose.

### *Thermogravimetric analysis*

The films obtained from plant husks are natural polymers consisting mainly of hemicellulose compounds having carbon and hydrogen network with multiple hydroxyl groups. The films of a husk of *Plantango ovate* (sample 1), *Cydonia oblonga* (sample

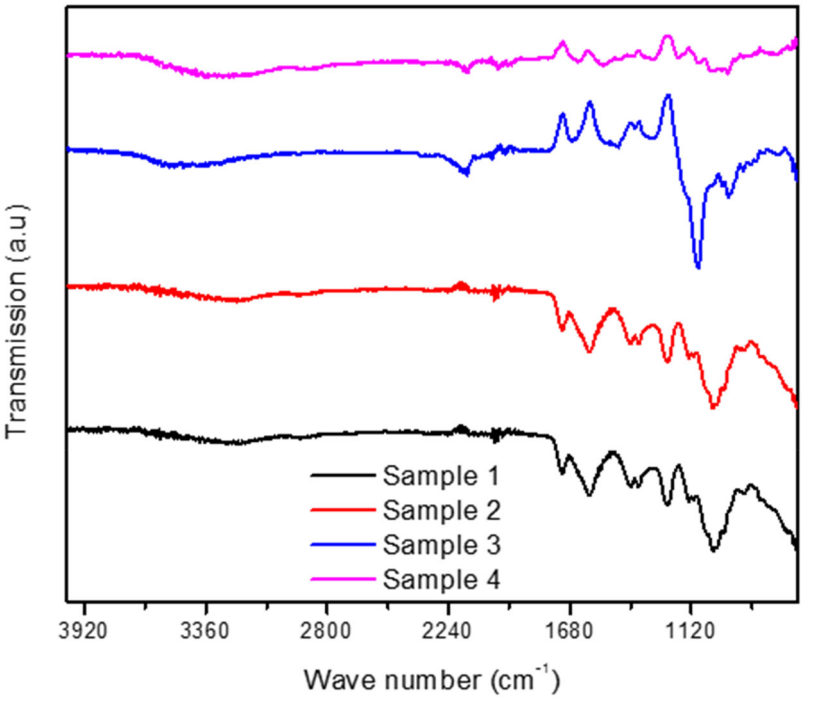


**Figure 3.** Thermogravimetric analysis of *Plantango ovate (1), Cydonia oblonga (2), Mimosa pudica (3), and Cochlospermum religiosum (4).*

2), *Mimosa pudica* (sample 3), and *Cochlospermum religiosum* (sample 4) were taken for the analysis.

All samples are similar in its chemical nature and almost shown similar peaks to depict percentage weight loss as shown in Figure 3. One major curve difference is 35.77% weight loss which we might be due to the decarboxylation and dihydroxylation. The lower minor curve indicates ash and hydrogen gas evolution which is 14.39%. This confirmed the composition of material which is only comprise of hemicelluloses. The glass transition temperature (Tg) is found between 250 to 300 Degree Celsius which make them thermally stable materials to resist the temperature variation in human body and made them compatible to be used as lens by providing longer shelf life, as drug binder by tuning for temperature and pH sensitivity and even in fiber optics for better conduction of signals.

## *Optical studies*

Optical studies of synthetic and natural polymers are mandatory for applications including optical fibers, packaging, electronics, photonics, and many more [42–48]. To deal with light-sensitive and light-transmitting features of polymers we need to have a particular set of optical parameters with a given range of optical properties. Although ophthalmologists have long been aware of the lethal effects of poor optical quality in spectacles lenses, there is still limited knowledge of the effects of the poor optical quality of contact lenses. Any abnormality in the refractive surface of the lens

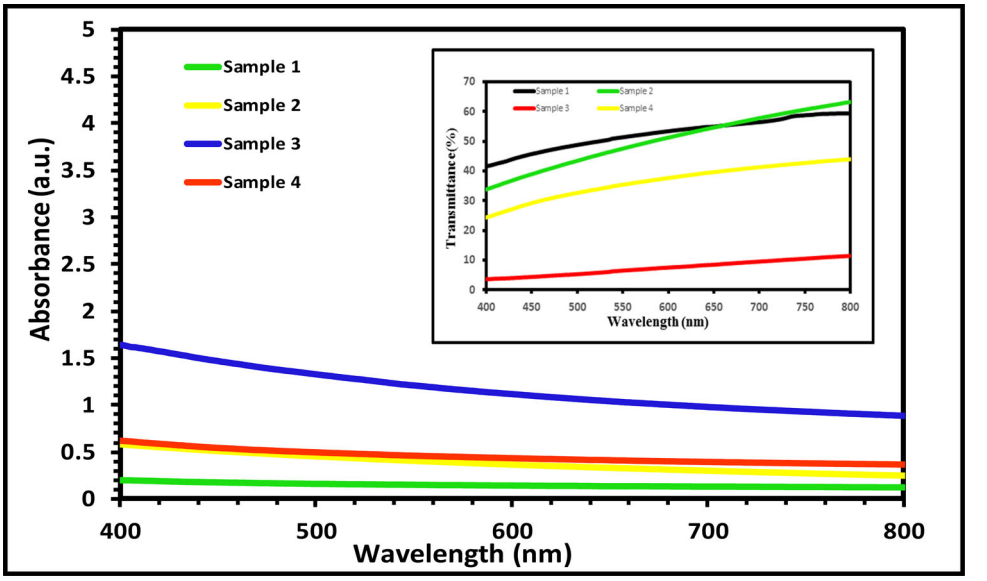


**Figure 4.** Inset graph of transmittance and absorption in Visible region of Plantango ovate *(a), Cydonia oblonga (b), Mimosa pudica (c), and Cochlospermum religiosum (d).*

cause variation in the shadow cast by the lens. Refractive index, transmittance, and dispersion energy are the most vital optical parameters required to be evaluated for materials to be used for optical applications. Some important optical parameters are discussed below.

### *UV-visible absorption and transmittance spectra*

Absorption and transmittance spectra of the husk of *Plantango ovate, Cydonia oblonga, Mimosa pudica,* and *Cochlospermum religiosum* are shown in Figure 3 The absorption bands around 280 nm for *Plantango ovate* and *Cydonia oblonga* while the absorption band at 340 nm for *Mimosa pudica* and *Cochlospermum religiosum* can be assigned to the transitions of n $\pi^*$ and $\pi$ $\pi^*$. No characteristic absorption band structure is observed in the visible region and also the absorption is very low in this region that can help us to conclude with the fact that hemicellulose films are transparent to the visible region as it is depicted in the graph of the UV region with Visible region as shown in Figure 4 From Figure 3, it is depicted that for transparent materials the absorption should be minimum and transmittance should be maximum. In this regard *Plantango ovate* is considered to be the most suitable natural polymer while *Cydonia oblonga* and *Mimosa pudica* both have quite comparable behavior which made them as potential substance to be used as translucent material. *Cochlospermum religiosum* shown relatively more absorption because it imparts light shade which make it to absorb more light. Although it is not crystal clear which make it suitable to be used as lens, but it is showing excellent features for rest of optical and thermal properties.

### Determination of optical energy band gap

The optical and electrical behavior of polymers can be explained by considering their bandgap. The optical band gap determines that what portion of solar spectrum any material could absorb. The optical absorption spectrum can be an important tool for the determination of such a bandgap. The absorption is caused by transitions between valence and conduction band states positioned near the respective mobility edges and is expressed by optical band gap energy ($E_g$). Mott and Devis [49,50] developed an equation as shown below which relates the absorption coefficient as a function of bandgap ($E_g$) and photon energy.

$$(\alpha h\nu) = B(h\nu - Eg)^m$$

In the above-mentioned equation, "B" is a constant and a factor that depends on transition probability whereas "m" is used to specify the type of electronic transition and is related to the distribution of density of the states. The "m" is an index describing the type of optical transition where it receipts the value $1/2$ for direct transition whereas for indirect transition m goes out to be 2 [45–49]. Here "α" is the absorption coefficient of the material, "$h\nu$" is the photon energy and "$E_g$" is bandgap energy. the value of $m = 1/2$ is for direct allowed transitions and $m = 2$ for indirectly allowed transitions. Direct as well as indirect band gaps are possible for *Plantango ovate, Cydonia oblonga, Mimosa pudica,* and *Cochlospermum religiosum.* $(\alpha h\nu)^{1/2}$ was plotted against independent variable photon energy (h$\nu$) to obtain an indirect bandgap. The plots of $(\alpha h\nu)^{1/2}$ versus the photon energy (h$\nu$) are shown in Figure 5 for the *Plantango ovate* (a), *Cydonia oblonga* (b), *Mimosa pudica* (c), and *Cochlospermum religiosum* (d). Extrapolation of the linear portion of the curve to the point $(\alpha h\nu)^{1/2} = 0$ gives the indirect optical energy bandgap. Such bandgap for *Plantango ovate* is 4.8 eV, for *Cydonia oblonga* it becomes 4.4 eV, *Mimosa pudica* estimated value is 3.9 eV and 3.9 eV for *Cochlospermum religiosum.* Yoshimichi Ohki reported that the bandgap energies vary with different functionalities of the polymers. It is rather high in linear polyolefin polymers such as 6.9 and 7.0 eV for polyethylene and polypropylene, respectively. However, the polymers with aromatic rings partake low band gap energies. Hemicellulose is neither contain olefin nor aromatic rings in their structure that is why their bandgap energy lies in between of both of these categories.

Whereas plot of $(\alpha h\nu)^2$ verses h$\nu$ was used to get the direct bandgap energy. The plots of $(\alpha h\nu)^2$ versus the photon energy are shown in Figure 6 for the *Plantango ovate* (a), *Cydonia aoblonga* (b), *Mimosa pudica* (c), and *Cochlospermum religiosum* (d). Extrapolation of the linear portion of the curve to the point $(\alpha h\nu/^2 = 0$ gives the direct optical energy bandgap. Such bandgap for *Plantango ovate* is 5.9 eV, for *Cydonia oblonga* it becomes 5.5 eV, *Mimosa pudica* estimated value is 4.6 eV and 5.4 eV for *Cochlospermum religiosum.*

It is evident that for each sample the direct bandgap energy is higher than indirect bandgap energy [46]. Direct and indirect bandgap energies are quite independent from each other.

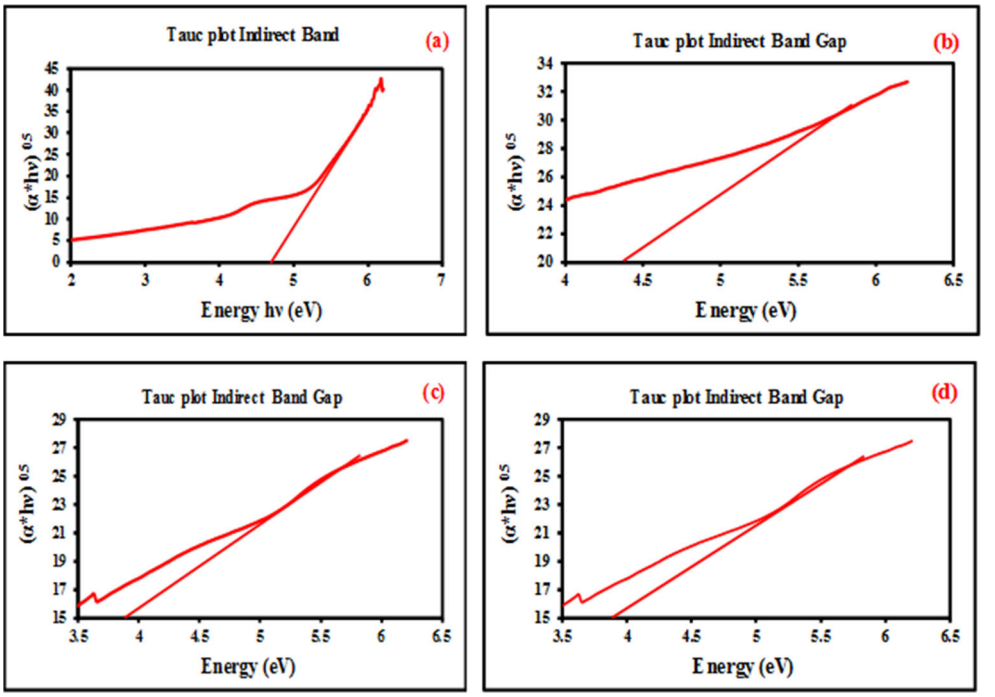


**Figure 5.** Plot of $(\alpha h\nu)^{1/2}$ vs. Energy *for Plantango ovate (a), Cydonia oblonga (b), Mimosa pudica (c), and Cochlospermum religiosum (d).*

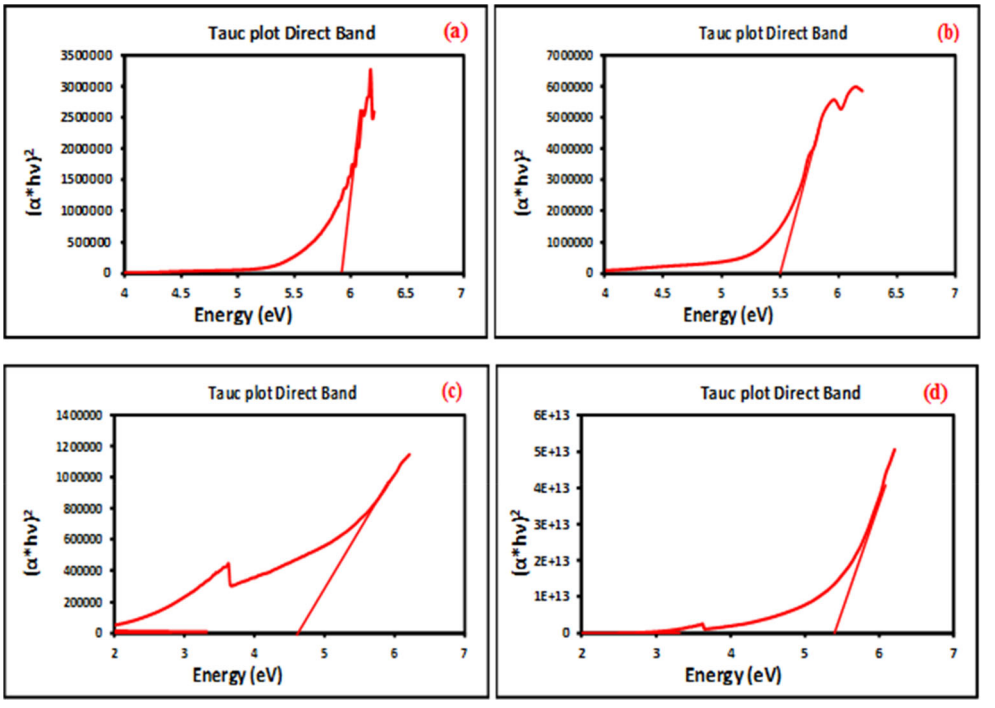


**Figure 6.** Plot of $(\alpha h\nu)^2$ vs. Energy for *Plantango ovate (a), Cydonia oblonga (b), Mimosa pudica (c), and Cochlospermum religiosum (d).*

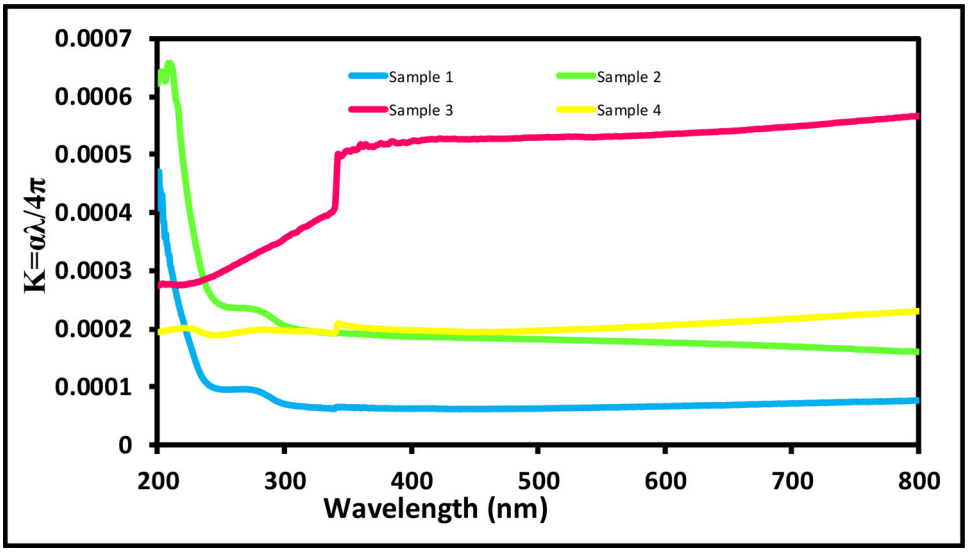


**Figure 7.** Variation of Extinction coefficient (K) with the change in wavelength of light *for Plantango ovate (a), Cydonia oblonga (b), Mimosa pudica (c), and Cochlospermum religiosum (d).*

## *Refractive index*

The Refractive index is also a significantly important physical parameter to assign the optical and electronic properties of the material system. The materials for optical and optoelectronic items are highly inclined by the nature and magnitude of such physical parameters [51]. High refractive index optical materials are needed in various fields including ophthalmic lenses, optical waveguides, LED encapsulation objects, anti-reflection films, and adhesives for optical components [42–47].

The Refractive indices are closely related to the structural features of polymeric materials. The refractive indices for the samples were determined by the following equation [45–47].

$$R = \frac{(n-1)^2 + K^2}{(n+1)^2 + K^2}$$

Where "R" is the reflectance and "K" is the extinction coefficient ($K = \alpha\lambda/4\pi$). The data for reflectance is from the values of absorbance (A) and transmittance (T) using the following equation [45–47].

$$T = (1-R)^2 \exp(-A)$$

Refractive index (n) and extinction coefficient (K) are shown in Figures 7 and 8. The Refractive index of any material is associated with the electronic polarization of the ions and local field inside of the material [51]. The electronic polarization increases with the frequency [52,53] therefore the RI also increases with the frequency.

In general, the behavior of refractive index (n) and extinction coefficient (K) follow the same pattern, the extinction coefficient (K) decreased with an increase in the wavelength except for *Mimosa pudica* (sample 3) which is also depicted through absorption

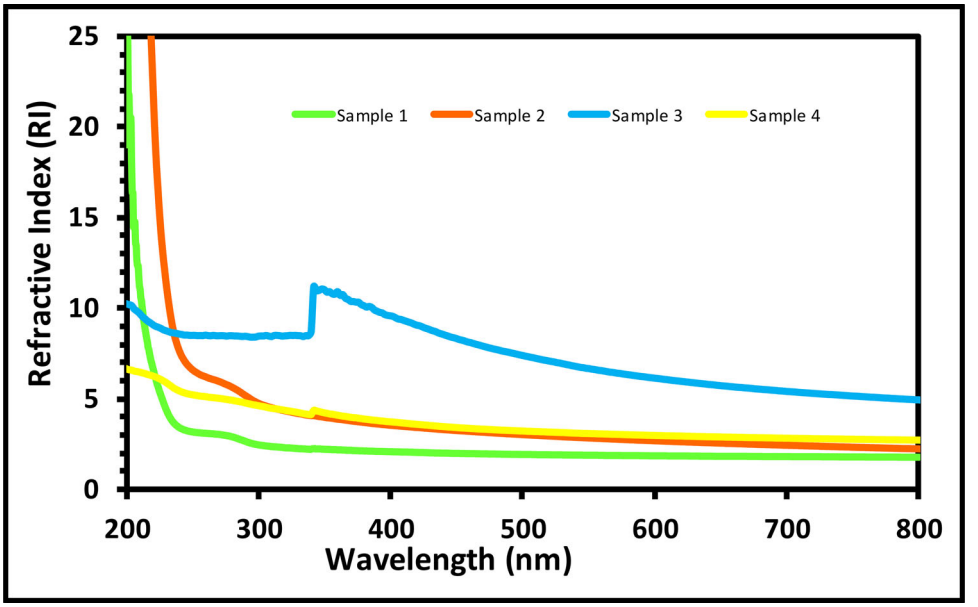


**Figure 8.** Variation of Refractive Index (n) with the change in wavelength of light for *Plantango ovate (a), Cydonia oblonga (b), Mimosa pudica (c), and Cochlospermum religiosum (d).*

spectrum, this variation is due to presence of slight shade and bit more thickness of the film in comparison to rest of the films while refractive index (n) decreases with the increase in wavelength for all the samples. The refractive index at 600 nm wavelength for *Plantango ovate* is 2.5, *Cydonia oblonga* is 3, *Mimosa pudica* is 5.2 and *Cochlospermum religiosum* possesses 3.75. The higher the value of the Refractive index, greater the time required to travel through that material. The variation of the refractive index is a property of dispersion that directly affects the functional properties of optical materials.

## Optical dispersion parameters

The dispersal of RI of polymeric films with maximum transparency region of wavelength has been examined in terms of the Wemple–Di Domenico single effective oscillator model [54]. Refractive index (n) as a function of wavelength was fitted to Wemple–Di Domenico single oscillator model; and the parameters like single oscillator energy ($E_o$), dispersion energy ($E_d$), average oscillator wavelength, and oscillator length were also evaluated, and the results are discussed. Wemple–Di Domenico model expressed the relation between the refractive index (n), Eo, and Ed by the following relation [54].

$$\frac{1}{n^2-1} = \frac{E_o}{E_d} - \frac{1}{E_o E_d}(h\nu)^2$$

Here, $E_o$ is the average excitation energy or oscillator energy gap for electronic transitions, and $E_d$ is the dispersion energy measuring the strength of inter-band optical transition [47] (Figure 9).

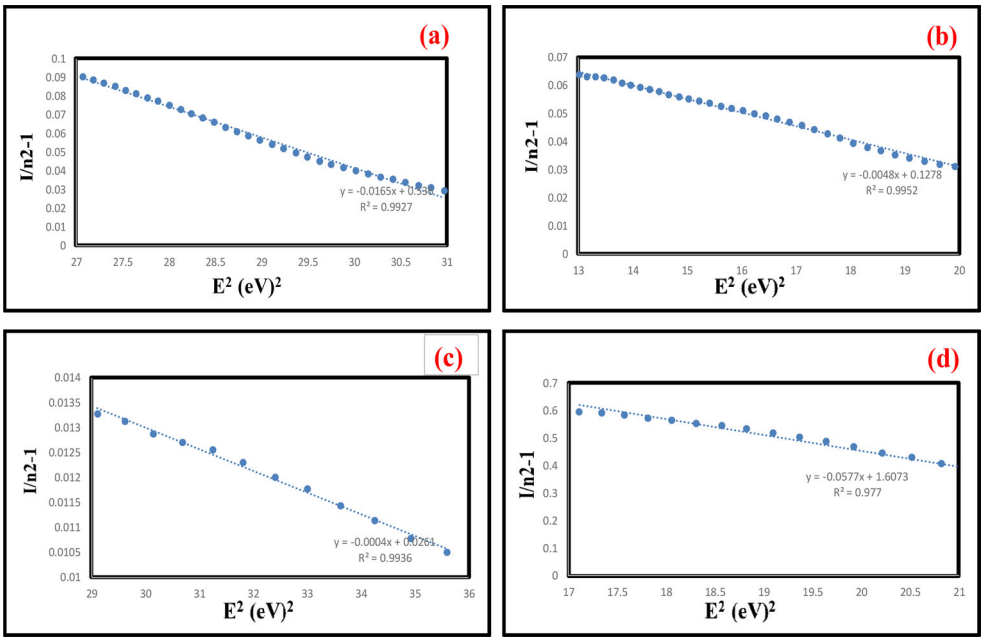


**Figure 9.** Plot of $(1/n^2\text{-}1)$ Vs $(\text{Energy})^2$ *Plantango ovate (a), Cydonia oblonga (b), Mimosa pudica (c), and Cochlospermum religiosum (d).*

$E_d$ and $E_o$ can directly be calculated from the intercept ($E_o/E_d$) and slope ($1/E_oE_d$) of the linear fitted lines by plotting1/(n2–1) versus $E^2$ shown in Figure 8 Actually, $E_d$ measures the average strength of the inter-band optical transitions and is related to the charge distribution, whereas $E_o$ measuring the average energy bandgap [30]. It may be noted that the value of the oscillator energy ($E_o$) follows the same trend with the optical energy bandgap ($E_g$) calculated from Eq. (2) for bandgap.

However, the calculated energy gaps from the W-D model are somewhat higher but reasonably close to that obtained from the energy band gap equation. Based on the concept of bandgap by Mott and Devis [49,50]. The evaluated values are summarized in Table 1.

As the wave-length ($\lambda$) depends on the refractive index, average inter-band oscillator wavelength ($\lambda_0$), the long-wavelength refractive index ($n_\infty$), and the average oscillator strength ($S_0$) for all the films are obtained from the following relations based on the single term Sellmeir oscillator [55].

$$\frac{1}{n^2-1} = \frac{1}{S_0\lambda_0} - \frac{1}{S_0}(\lambda^{-2})$$

The parameters $S_o$ and $\lambda_o$ were obtained from the intercept and the slope of the linear fitted plot [56] of $1/n^2\text{-}1$ against $\lambda^{-2}$ as shown in Figure 10. The values obtained from these curves correspond with the absorption edges obtained from UV-Vis spectra.

**Table 1.** Different optical parameters.

| Samples | $S_o$ | $\lambda_o$ | $E_o$ | $E_d$ |
|---|---|---|---|---|
| Sample 1 | 3.966 | 1.3440 | 9.2537 | 1.7264 |
| Sample 2 | 1.342 | 4.8530 | 1.2584 | 9.8466 |
| Sample 3 | 1.660 | 1.5312 | 8.0982 | 3.1750 |
| Sample 4 | 8.548 | 2.3307 | 5.3744 | 5.1800 |

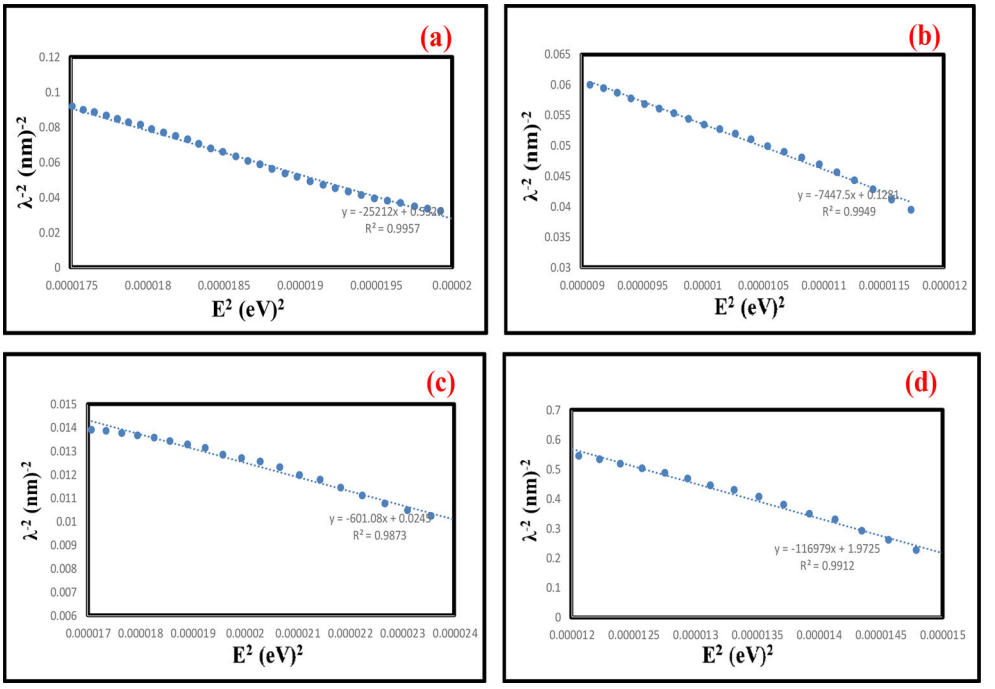


**Figure 10.** The plot of (Wavelength)$^2$ Vs (Energy)$^2$ *Plantango ovate (a), Cydonia oblonga (b), Mimosa pudica (c), and Cochlospermum religiosum (d).*

## *Optical conductivity*

The optical conductivity ($\sigma$) is an important characteristic of the material to consider its electronic states. The optical conductivity is represented by $\boldsymbol{\sigma}$.

$$\boldsymbol{\sigma} = \frac{\boldsymbol{\alpha nc}}{4\boldsymbol{\pi}}$$

According to this relationship, optical conductivity is related to the basic energy band structure of the material. Where "α" is the absorption coefficient and "c" is the velocity of light while n is the refractive index [47,48].

Optical conductivity is the function of wavelength as shown in Figure 11. Where it has dimensions of frequency. Optical conductivity was found to be decreased with an increase in wavelength in the visible range of this study (400-800 nm). The value of the optical conductivity at 600 nm is selected as the backdrop because 600 nm is the average of the visible range are obtained as $2 \times 10^{10}$ for *Plantango ovate*, $3.5 \times 10^{10}$ for

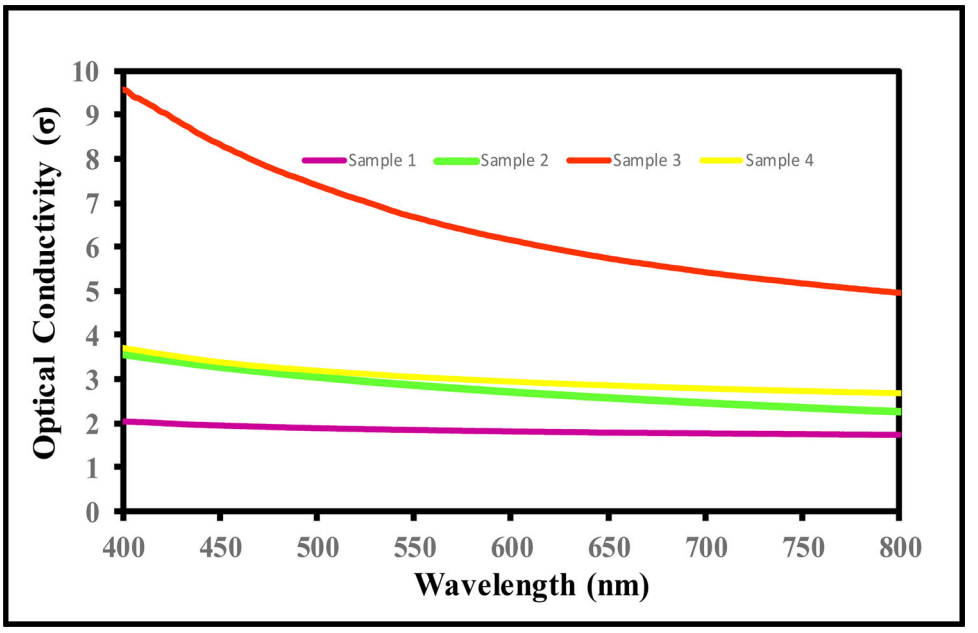


**Figure 11.** Optical conductivity vs Wavelength for *Plantango ovate (1), Cydonia oblonga (2), Mimosa pudica (3), and Cochlospermum religiosum (4).*

*Cydonia oblonga,* $9.5 \times 10^{10}$ for *Mimosa pudica,* and $3.75 \times 10^{10}$ for *Cochlospermum religiosum.* Thus at 6 nm, the optical conductivity is relatively highest for *Mimosa pudica (sample 3). As it depends on the nature of the material and the absorption coefficient and for Mimosa pudica the value of* α is high that's why it is showing more optical conductivity *while the optical conductivity is quite comparable for Cydonia oblonga and Cochlospermum religiosum* and least for *Plantango ovate.*

## Determination of urbach energy

The defect level of an optical material can be determined by the value of Urbach Energy. From the absorption spectrum, it is revealed that the spectrum ends towards the low-energy side below the band edge. These can be ascribed to the transition from localized states in the valence band to the conduction band. Additives or defects are the reason for localized states [57]. For amorphous materials, Urbach energy can be calculated by using the following equation.

$$\alpha(\nu) = \alpha_0 \ exp \ (h\nu/E_u)$$

Where $E_u$ is Urbach energy which depends on the width of the localized states in the optical bandgap. and $\alpha_0$ is a constant. The values of ln$\alpha$ verses h$\nu$ are plotted and shown in Figure 12. The value of $E_u$ can be calculated by the inverse of the slope. It explains the defect level of in optical band gap of the films. The value of $E_u$ for *Plantango ovate* is 2.9 eV, *Cydonia oblonga* is 2.1 eV, *Mimosa pudica* is 1.6 eV and *Cochlospermum religiosum* possesses 5.6 eV. According to $E_u$ values *Mimosa pudica* is the most pertinent material for optical applications while it is least suitable for the

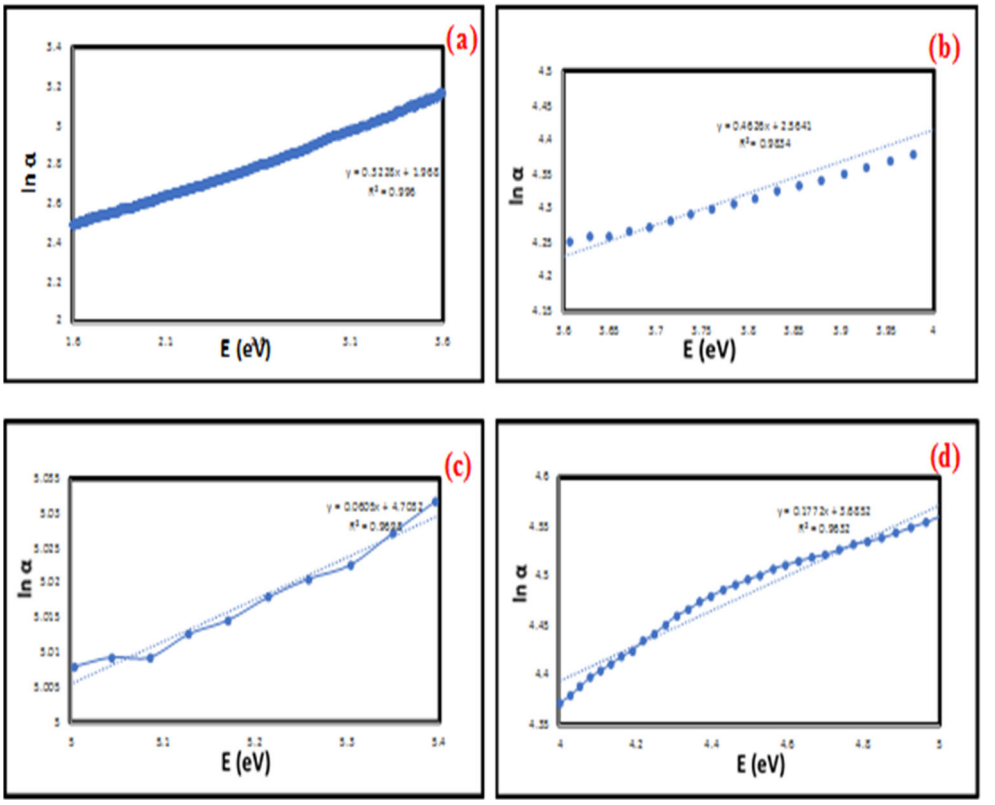


**Figure 12.** Plots of lnα vs. energy (eV) for *Plantango ovate (a), Cydonia oblonga (b), Mimosa pudica (c), and Cochlospermum religiosum (d).*

synthesis of contact lenses similarly *Cochlospermum religiosum* possess least potential for optical devices while rest of the materials are quite appropriate to be used as a potential raw material for contact lens synthesis and to use as a drug binder or to show good adsorption capabilities to remove metal ions.

Comparatively the $E_u$ (Urbach energy) value is lower than the $E_g$ (bandgap energy) or $E_0$ (dispersion energy) values. Thus, it is also evident that $E_g$ (bandgap energy) values are lower than $E_0$ (dispersion energy) values but higher than $E_u$ (Urbach energy) values.

It can also be observed that disorder in optical material affects the band gap regardless of the type or nature of the defect [57].

## Conclusion

Films of a pure husk of *Plantango ovate, Cydonia oblonga, Mimosa pudica, Cochlospermum religiosum* were prepared and proteins, lignin, and cellulose was removed to make transparent films for a variety of applications. Thermal analysis indicates that obtained material is quite stable substance and can sustain high temperature as their Tg is around 250 to 300 °C. Spectral information reveals that these are transparent materials with minimum absorption and maximum transmittance.

The optical studies indicate that both the direct and indirect bandgap of each of the natural polymers are comparable. The purity of the extracted substances have high optical conductivity and a good refractive index. Optically, these natural polymers are suitable to possess noteworthy values of dispersion and Urbach energy. In recent times researchers are in search of understanding how disorder influences the optical absorption spectrum of a material system. This paper is an effort to understand how the thermal and structural components of the disorder within these natural polymeric films contribute to the optical properties of the films. These results are quite informative and interesting and might help to observe their applications not only from fiber optics to transparent contact lens materials but also for their use as drug binder and adsorptive biomass to remove heavy metals from organic dyes to industrial effluents.

## Acknowledgments

We like to acknowledge Dr. Tariq Qamar Assistant Professor FCCU for his guidance and support in experimentation and characterizations.

## Disclosure statement

No potential conflict of interest was reported by the author(s).

## References

[1] Urbach F. The long-wavelength edge of photographic sensitivity and the electronic absorption of solids. Phys Rev. 1953;92(5):1324–1324.
[2] Elias HG, Weinheim VCH. An intro. to plastics. Polymer Inter. 1993;34:237–238.
[3] Migahed MD, Zidan HM. Influence of UV-irradiation on the structure and optical properties of polycarbonate films. Curr Appl Phys. 2006;6(1):91–96.
[4] Bhajantri RF, Ravindrachary V, Harisha A, et al. Microstructural studies on BaCl2 doped poly (vinyl alcohol). Polymer. 2006;47(10):3591–3598.
[5] Sachdev P, Banerjee M, Mukherjee GS. Effect of Ag underlayer on structural and optical properties of PVA/Ag/Co film. DSJ. 2014;64(3):290–294.
[6] Banerjee M, Sachdev P, Mukherjee GSJ. Exchange bias and bistable magneto-resistance states in amorphous TbFeCo thin films. Appl Phys. 2012;111(9):094302.
[7] Banerjee M, Sachdev P, Mukherjee GS. Studies on magnetic nanocomposites of carbon cobalt vinyl-polymer prepared by ion beam sputtering technique. J Sci Conf Proc. 2009; 1(1):86–92.
[8] Uemura T, Dong J, Wang Y, et al. Transplantation of cultured bone cells using combinations of scaffolds and culture techniques. Biomaterials. 2003;24(13):2277–2286.
[9] Fragonas E, Valente M, Pozzi-Mucelli M, et al. Articular cartilage repair in rabbits by using suspensions of allogenic chondrocytes in alginate. Biomaterials. 2000;21(8): 795–801. [10721748]
[10] Jiang T, Abdel-Fattah WI, Laurencin CT. In vitro evaluation of chitosan/poly(lactic acid-glycolic acid) sintered microsphere scaffolds for bone tissue engineering . Biomaterials. 2006;27(28):4894–4903.
[11] Dias GJ, Peplow PV, Teixeira F. Osseous regeneration in the presence of oxidized cellulose and collagen. J Mater Sci Mater Med. 2003;14(9):739–745.
[12] Ongpipattanakul B, Nguyen T, Zioncheck TF, et al. Development of tricalcium phosphate/amylopectin paste combined with recombinant human transforming growth factor-beta 1 as a bone defect filler. J Biomed Mater Res. 1997;36(3):295–305.

[13] Vogelin E, Jones NF, Huang JI, et al. Healing of a critical-sized defect in the rat femur with use of a vascularized periosteal flap, a biodegradable matrix, and bone morphogenetic protein. J. Bone Joint Surg. Am. 2005; 87 :1323–1331.
[14] Peppas N, Bures P, Leobandung W, et al. Hydrogels in pharmaceutical formulation. Eur J Pharm Biopharm. 2000;50(1):27–46.
[15] Tønnesen HH, Karlsen J. Alginate in drug delivery systems. Drug Dev Ind Pharm. 2002;28(6):621–630.
[16] Xian C, Yuan Q, Bao Z, et al. Natural polymer-based hydrogels with enhanced mechanical performances: preparation, structure, and property. Adv Healthcare Mater. 2019; 8(17):1900670.
[17] Carter P, Narasimhan B, Wang Q. Biocompatible nanoparticles and vesicular systems in transdermal drug delivery for various skin diseases. Int J Pharm. 2019;555:49–62.
[18] Wei X, Liao J, Davoudi Z, et al. Folate receptor-targeted and GSH-responsive carboxymethyl chitosan nanoparticles containing covalently entrapped 6-mercaptopurine for enhanced intracellular drug delivery in Leukemia. Mar Drugs. 2018;16(11):439.
[19] Deretic V, Gill J, Chakrabarty A. Alginate Biosynthesis: A model system for gene regulation and function in *Pseudomonas*. Bio/Technol. 1987;5:469–477.
[20] Li Z, Ramay HR, Hauch KD, et al. Chitosan-alginate hybrid scaffolds for bone tissue engineering. Biomaterials. 2005;26(18):3919–3928. [15626439]
[21] Huang K, Wu J, Gu Z. Black phosphorus hydrogel scaffolds enhance bone regeneration via a sustained supply of calcium-free phosphorus. ACS Appl Mater Interfaces. 2019; 11(3):2908–2916.
[22] Brown JQ, Srivastava R, McShane MJ. Encapsulation of glucose oxidase and an oxygen-quenched fluorophore in polyelectrolyte-coated calcium alginate microspheres as optical glucose sensor systems. Biosens Bioelectron. 2005;21(1):212–216.
[23] Whitchurch CB, Alm RA, Mattick JS. The alginate regulator Alg R and an associated sensor FimS are required for twitching motility in Pseudomonas aeruginosa. Proc Natl Acad Sci USA. 1996;93(18):9839–9843.
[24] Rashid A, Graham AN. United States patent. no. 14/621316. Ocutec Ltd, Bellshill (GB). the United States patent application publication; 2015.
[25] Dafe A, Etemadi H, Dilmaghani A, et al. Investigation of pectin/starch hydrogel as a carrier for oral delivery of probiotic bacteria. Int J Biol Macromol. 2017;97:536–543.
[26] Huang J, Huang K, You X, et al. Evaluation of tofu as a potential tissue engineering scaffold. J Mater Chem B. 2018;6(9):1328–1335.
[27] Liu G, Zhou H, Wu H, et al. Preparation of alginate hydrogels through solution extrusion and the release behavior of different drugs. J Biomater Sci Polym Ed. 2016;27(18): 1808–1823.
[28] Liu G, Yuan Q, Hollett G, et al. Cyclodextrin-based host-guest supramolecular hydrogel and its application in biomedical fields. Polym Chem. 2018;9(25):3436–3450.
[29] Ren K, Cui H, Xu Q, et al. Injectable polypeptide hydrogels with tunable microenvironment for 3D spreading and chondrogenic differentiation of bone-marrow-derived mesenchymal stem cells. Biomacromolecules. 2016;17(12):3862–3871.
[30] Schexnailder P, Schmidt G. Nanocomposite polymer hydrogels. Colloid Polym Sci. 2009;287(1):1–11.
[31] Cui H, Zhuang X, He C, et al. AIE supramolecular assembly with FRET effect for visualizing drug delivery. Acta Biomater. 2015;11:23840–23847.
[32] Ishihara M, Nakanishi K, Ono K, et al. Photocrosslinkable chitosan as a dressing for wound occlusion and accelerator in healing process. Biomaterials. 2002;23(3):833–840.
[33] Murakami K, Aoki H, Nakamura S, et al. Hydrogel blends of chitin/chitosan, fucoidan and alginate as healing-impaired wound dressings . Biomaterials. 2010;31(1):83–90. [19775748]
[34] Ahrens CC, Welch ME, Griffith LG, et al. Uncharged helical modular polypeptide hydrogels for cellular scaffolds. Biomacromolecules. 2015;16(12):3774–3783.

[35] Madl CM, Katz LM, Heilshorn SC. Tuning bulk hydrogel degradation by simultaneous control of proteolytic cleavage kinetics and hydrogel network architecture. Adv Funct Mater. 2016;26(21):3612–3620.
[36] Lane DD, Fessler AK, Goo S, et al. Sustained tobramycin release from polyphosphate double network hydrogels. Acta Biomater. 2017;50:484–492.
[37] Wu J, Zhao X, Wu D, et al. Development of a biocompatible and biodegradable hybrid hydrogel platform for sustained release of ionic drugs. J Mater Chem B. 2014;2(38):6660–6668.
[38] Ngwabebhoh FA, Gazi M, Oladipo AA. Microwave-assisted synthesis of high-performance polymer-based nano adsorbents for pollution control. Chem Eng Res Des. 2016; 112:200–241.
[39] Felipe D, Marjory L, José R, et al. Physicochemical properties of edible seed hemicelluloses. OALib J. 2017;4:1–14.
[40] Egüés I, Sanchez C, Mondragon I, et al. Effect of alkaline and autohydrolysis processes on the purity of obtained hemicelluloses from corn stalks. Bioresour Technol. 2012; 103(1):239–248.
[41] Lisong H, Menghao D, Jinping Z. Hemicellulose-based hydrogels present status and application prospects: A brief review. J Forestry. 2018;8:1.
[42] Vishnu M, Gyan P, Mala R. Value-added products from hemicelluloses: Biotechnological perspective. Div Biochem Sci. 2015;4:1. NCL.
[43] Ayedta I, Illarramendi MA, Arrue J, et al. Optical characterization of doped thermoplastic and thermosetting polymer-optical-fibers. Polymers. 2017; 9:90.
[44] Cui Z, Lü C, Yang B, et al. Research on preparation, structure, and properties of TiO2/polythiourethane hybrid optical films with high refractive index. Macromol Mater Eng. 2003;288(9):717–723.
[45] Rozra J, Saini I, Sharma A, et al. Investigation of zinc oxide-loaded poly (vinyl alcohol) nanocomposite films in tailoring their structural, optical and mechanical properties. Mater Chem Phys. 2012;47:3912–3926.
[46] Bhargav P, Mohan V, Sharma AK, et al. Structural, electrical and optical characterization of pure and doped poly (vinyl alcohol) (PVA) polymer electrolyte films. Int J Polym Mater. 2007;56(6):579–591.
[47] Abdullah OG, Aziz SB, Omer KM, et al. In-situ Synthesis of PVA/HgS nanocomposite films and tuning optical properties. J Mater Sci Mater Electron. 2015;26(7):5303–5309.
[48] Wongpaibool V. Optical Fibre Characteristics and System Configurations," VirginiaTech, Dissertation, Improvement of fiber optic system performance by Synchronous phase Modulation and filtering at the Transmitter. 2018.
[49] Mott NF, Devis NF. Electronic process in noncrystalline materials. 2nd ed. Oxford: Oxford University Press; 1979; p. 273.
[50] Tauc J. Optical properties of solid. Abeles F, editor. Amsterdam: North-Holland; 1972; p. 277–313.
[51] Banerjee M, Jain A, Mukherjee GS. Microstructural and optical properties of polyvinyl alcohol/manganese chloride composite film. Polym Compos. 2019;40(S1):E765–775.
[52] Van Vlack LH. Elements of materials science and engineering. 6th ed. Michigan: Wiley, Addition-Wesley Publishing Company; 1989. p. 469.
[53] Umesh K. Optical properties of polycrystalline zinc selenide thin films. Sci Res J. 2012; 3:36–40.
[54] Wemple SH, DiDomenico M. Behavior of the electronic dielectric constant in covalent and ionic materials. Phys Rev B. 1971;3(4):1338–1351.
[55] Joshi JH, Khunti DD, Joshi MJ, et al. *AIP Conference Proceedings*, 2017, 04003.
[56] Saini I, Rozra J, Chandak N, et al. Tailoring of electrical, optical, and structural properties of PVA by addition of Ag nanoparticles. A Mater Chem Phys. 2013;139(2–3):802–810.
[57] Ayik C, Studenyak I, Kranjec M, et al. Urbach rule in solid state physics. Optics. 2014; 4(3):76–83.